Far-infrared vibrational mode in $Cu_{1-x}M_xGe_{1-y}Si_yO_3$ (M=Zn,Cd,Ni)

J. J. McGuire and T. R$\tilde{o}\tilde{o}$m*
Department of Physics and Astronomy, McMaster University, Hamilton, Ontario, Canada L8S 4M1

T. E. Mason
Department of Physics, University of Toronto, Ontario, Canada M5S 1A7

T. Timusk
Department of Physics and Astronomy, McMaster University, Hamilton, Ontario, Canada L8S 4M1

H. Dabkowska
Brockhouse Institute for Materials Research, McMaster University, Hamilton, Ontario, Canada L8S 4M1

S. M. Coad and D. McK. Paul
Department of Physics, University of Warwick, Coventry CV4 7AL, United Kingdom
(Received 19 August 1998)

We report on far-infrared measurements of Zn-, Cd-, and Ni-doped crystals of the spin-Peierls compound $CuGeO_3$. Dopants that replace Cu have the effect of introducing several absorption lines, polarized in the ab plane, between 5 and 55 cm^{-1}. The intensity of the absorption grows with dopant concentration but saturates above 2%. One line near 10 cm^{-1} loses intensity above 4 K, and a second line near 20 cm^{-1} is absent at low temperatures but grows to peak at about 40 K in agreement with a three-level model with two excited states 10 and 30 cm^{-1} above the ground state. As the doping is increased these lines broaden and a temperature-independent absorption develops over the entire range from 5 to 55 cm^{-1}. These features are magnetic-field independent up to 16 T and are absent in samples doped with Si that replaces Ge instead of Cu. We suggest the new absorption is due to localized lattice modes of the dopant ion and the surrounding GeO_4 tetrahedra. [S0163-1829(99)05202-9]

The quasi-one-dimensional antiferromagnet $CuGeO_3$ is the first inorganic compound to show a spin-Peierls (SP) transition.[1] At $T=14$ K a gap opens in the excitation spectrum of the Cu $S=\frac{1}{2}$ spins as a result of magnetoelastic coupling. In general, such transitions involve a lowering of magnetic energy at the expense of lattice energy. Structures where large tightly bound blocks can move as units, such as the organic charge-transfer complexes, exhibit the spin-Peierls phenomenon. Similar structural units occur in oxides in the form of rigid AlO_4 or SiO_4 tetrahedra bonded weakly to each other to form easily distorted structures.[2] It has been found that in $CuGeO_3$ the SP transition involves both a dimerization of the copper ions along the **c** axis and a rotation of the GeO_4 tetrahedra about the **c** axis.[3] In this paper we present the results of a far-infrared transmission study of Zn-, Cd-, and Ni-doped $CuGeO_3$. Our results show that substitution for Cu induces new absorption lines near 10 and 20 cm^{-1}. By doing a detailed study of the Zn-doped system, we show that these transitions result from a very unusual, highly anharmonic localized vibrational mode involving the GeO_4 tetrahedra.

The lattice structure of $CuGeO_3$ is shown in Fig. 1. It consists of chains of relatively rigid GeO_4 tetrahedra along the **c** axis. Cu^{2+} ions are positioned between these chains and form chains of CuO_6 octahedra that share the GeO_4 oxygens. Adjacent octahedra share two oxygens that provide a superexchange path for the antiferromagnetic interaction between Cu^{2+} ions.

The far-infrared absorption spectrum of pure $CuGeO_3$ has a weak absorption line[4] in the SP phase at 44 cm^{-1} that corresponds to the SP gap energy ($\approx$5.5 meV) at $\mathbf{Q}=[0,0,0]$ of the magnetic Brillouin zone as determined by electron-spin resonance.[5] The line splits in a magnetic field as expected for a transition from the ground singlet state to the excited triplet state. The other low-lying spectral feature is a line at 48 cm^{-1} that has been identified as a weak B_{3u} phonon that corresponds to a displacement of the four planar oxygens in the direction of the apical oxygens in the CuO_6 octahedra.[6]

Doping of $CuGeO_3$ is particularly interesting because it results in an antiferromagnetic (AF) phase that seems to coexist with the SP phase in a range of temperatures and doping levels.[7–16] There are few measurements of the far-

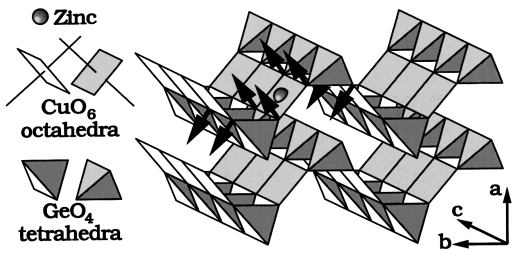

FIG. 1. Lattice structure of $CuGeO_3$. Arrows show possible motion of the rigid GeO_4 tetrahedra associated with a Zn-induced local vibrational mode.

infrared spectra of the doped systems of $CuGeO_3$ (Refs. 17 and 18) and, to our knowledge, none below 20 cm^{-1}.

We studied several single crystals including an undoped sample, a Cd-doped sample $Cu_{0.999}Cd_{0.001}GeO_3$, a Si-doped sample $CuGe_{0.997}Si_{0.003}O_3$, a Ni-doped sample $Cu_{0.98}Ni_{0.02}GeO_3$, and a series of Zn-doped samples $Cu_{1-x}Zn_xGeO_3$ with $x=0.003$, 0.01, 0.02, and 0.05. The Néel and SP transition temperatures, T_N and T_{SP}, were determined from magnetic susceptibility measurements on the same crystals. The $x=0.01$, 0.02, and undoped samples were grown by a floating-zone technique and the $x=0.001$, 0.003, and 0.05 samples by a self-flux method. We used either atomic-emission spectroscopy or mass spectroscopy to determine the dopant concentrations and found good agreement with phase diagrams[8,11,12,15,16] for T_{SP} and T_N vs concentration x.

The far-infrared measurements were done with a home-built polarizing Fourier spectrometer[19] and a new magnet insert with an *in situ* ^{3}He cooled ($T=0.3$ K) silicon bolometer. Polarization-dependent transmission measurements were done in magnetic fields up to 16 T from 3 to 100 cm^{-1} and in the temperature range from 1.2 to 100 K. Sample sizes were about $0.6\times2.5\times4$ mm^3 in the directions of the **a**, **b**, and **c** crystallographic axes,[20] respectively. The **k** vector of the light was aligned along the **a** axis (**k**$\|$**a**). To establish the symmetry of the transitions, additional measurements were done with **k**$\|$**b** for one of the Zn-doped samples ($x=0.01$). The dc magnetic field was in the direction of light propagation (Faraday geometry), and most of the spectra were measured at 1 cm^{-1} resolution. To calculate the absorption coefficient α from the transmittance it is necessary to estimate the refractive index. We used the interference fringes from a thin sample with parallel faces to do this. A constant value of $n=3$ was determined for the entire range from 3 to 100 cm^{-1}.

The absorption spectra for several samples at 1.2 K are shown in Fig. 2. The sample doped with $x=0.003$ Si is very similar to the undoped sample (not shown) in that the only far-infrared features are the lines at 44 and 48 cm^{-1}. In contrast, the $x=0.003$ Zn sample shows, in addition to these features, a line at 10 cm^{-1} that is not present in the Si-doped sample (or in the undoped samples). Increased doping results in a broadening of the 10-cm^{-1} line and the development of a broad absorption band between 5 and 55 cm^{-1}. The variation of the spectral weight[21] from 3 to 60 cm^{-1} (background and phonon line subtracted) is shown in the inset to Fig. 2 as a function of concentration. The dependence on Zn concentration appears to be linear at low concentrations but quickly saturates above $x=0.02$.

Absorption spectra for the $x=0.003$ Zn-doped sample were also obtained at higher temperatures. While the shoulder at 44 cm^{-1} disappears above the SP transition temperature as expected, the 10-cm^{-1} line and another line at 20 cm^{-1} show a temperature dependence that has no obvious relationship to the SP transition. The spectra are shown in the upper panel of Fig. 3, and the lower panel shows the spectral weight of the 10- and 20-cm^{-1} lines as functions of temperature. The 10-cm^{-1} line loses intensity as temperature is increased, but the 20-cm^{-1} line, which is absent at low temperatures, grows in intensity to peak around 40 K. Both

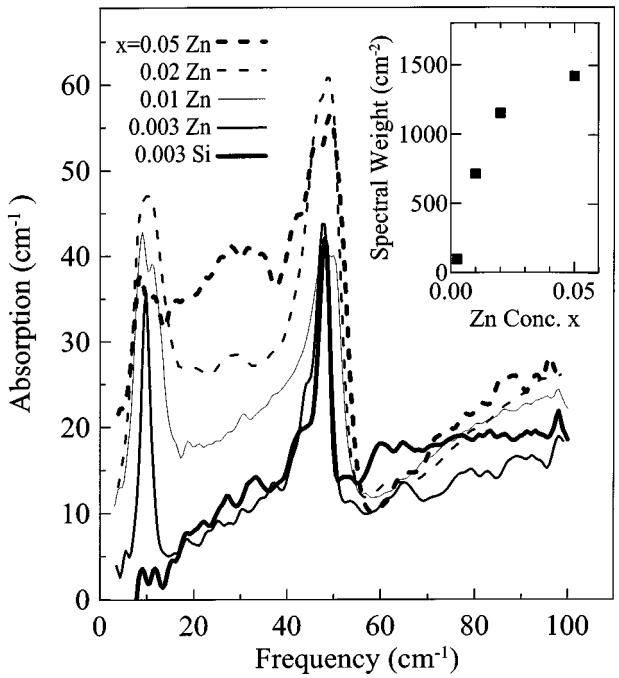

FIG. 2. Doping dependence of far-infrared absorption of $CuGeO_3$ crystals at 2 K with *b* polarization and **k**$\|$**a**. The inset shows spectral weight from 3 to 60 cm^{-1} as a function of Zn concentration. The spectral weight does not include the background that is taken to be the Si-doped sample spectrum.

lines shift to higher frequencies with temperature (inset to Fig. 3), and the 20-cm^{-1} line broadens significantly. Although the 10- and 20-cm^{-1} lines are broader in the more highly doped samples, they still show this temperature dependence. The broad absorption from 5 to 55 cm^{-1} in samples with $x>0.003$ is temperature independent up to 100 K, and we see no difference between spectra above and below the Néel temperature which can be attributed to the antiferromagnetic transition.

The temperature dependence of the 20-cm^{-1} line suggests that it is a transition from an excited state. A simple three-level model with two excited states 10 and 30 cm^{-1} above the ground state accounts for the temperature dependences of the line intensities in the lower panel of Fig. 3. The trends in the data are correctly reproduced, and the quality of the fit, though not particularly good, can be improved by adding higher energy levels to the model. This points to a multilevel, very anharmonic excitation, which is made possible by the replacement of a Cu^{2+} ion with Zn^{2+}, but not by the substitution of Si for Ge.

The polarization dependence of the new features was also obtained. With **k**$\|$**a**, the 10- and 20-cm^{-1} lines as well as the 5–55-cm^{-1} band were strongest when the electric field was along the **b** axis (*b* polarization) and nearly absent with *c* polarization. When the $x=0.01$ Zn sample was oriented with **k**$\|$**b**, the features were strongest with *a* polarization. Thus, if these are magnetic dipole transitions, they require that the magnetic-field component of the light is along the **c** axis. If they are electric dipole transitions, the electric field must be in the *ab* plane and have components both in the **a** and **b** directions.

To exclude magnetic dipole transitions we compare the

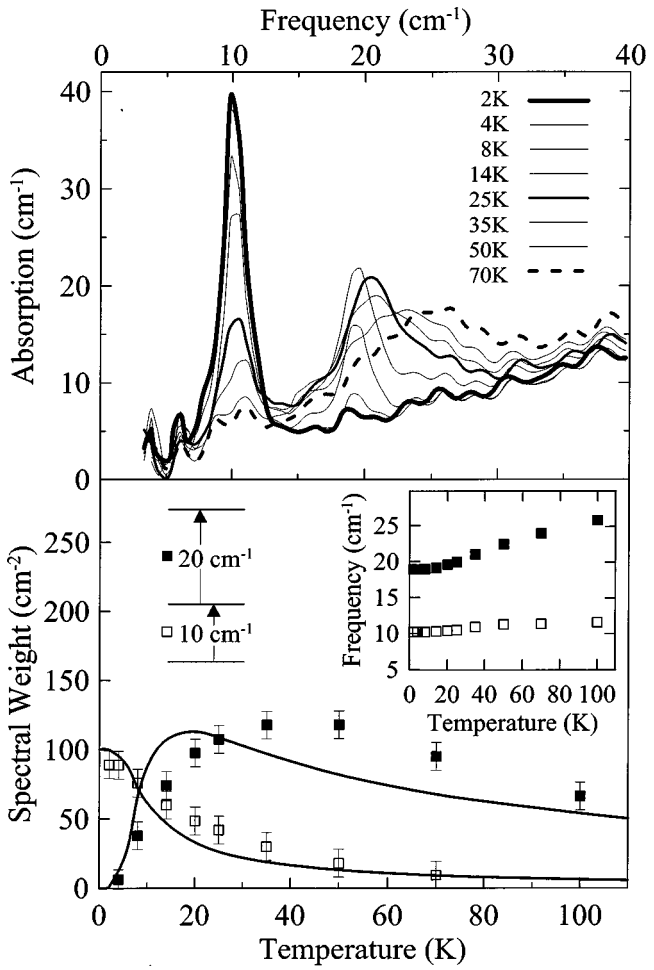

FIG. 3. Temperature dependence of 10- and 20-cm^{-1} lines in the $x=0.003$ Zn-doped sample. The upper panel shows absorption at various temperatures with *b* polarization and $\mathbf{k}\|\mathbf{a}$. The lower panel shows the spectral weight of the lines calculated using Lorentzian fits with frequencies shown in the inset. Solid lines are fits to the simple three-level model: $I_{10}(T)=A_{10}(1-e^{-\Delta_{10}\beta})/(1+e^{-\Delta_{10}\beta}+e^{-(\Delta_{10}+\Delta_{20})\beta})$, $I_{20}(T)=A_{20}e^{-\Delta_{10}\beta}(1-e^{-\Delta_{20}\beta})/(1+e^{-\Delta_{10}\beta}+e^{-(\Delta_{10}+\Delta_{20})\beta})$, where Δ_{10} and Δ_{20} are the temperature-dependent transition frequencies (inset), $A_{10}=100$ and $A_{20}=500$ are adjustable parameters, and $\beta=(k_BT)^{-1}$.

spectral weight of the Zn-induced absorption with that of a known magnetic-dipole transition in our system. An incommensurate phase exists in $CuGeO_3$ above $B_0\approx 12$ T (Refs. 22 and 23) where a magnetic dipole transition in the triplet ground state can be observed.[4] We find this transition (at 15 cm^{-1} in Fig. 4) to be independent of polarization in the *bc* plane ($B_0=15$ T along the **a** axis) as expected for an $S=1$, $\Delta M=\pm 1$ transition and to have a spectral weight of 2.5 cm^{-2}. The spectral weight of the 10-cm^{-1} line is 100 cm^{-2}, a factor of 40 larger than the magnetic-dipole transition. This discrepancy, which is even larger if we include the dilution due to low-Zn concentration, in combination with the fact that the frequency of the Zn-induced absorption is not affected by magnetic field up to 16 T, leads us to conclude that it is not a magnetic-dipole transition.

We can also rule out forbidden electronic electric-dipole transitions such as the transition in the SP phase from the singlet ground state to the excited triplet state that produces

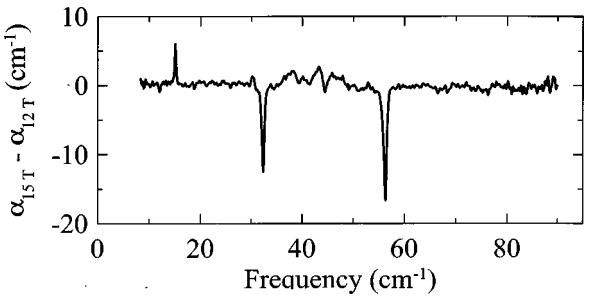

FIG. 4. Absorption in the SP phase at 12 T (negative features) subtracted from absorption in the incommensurate phase at 15 T (positive features) for the undoped sample at 2.1 K and 0.2 cm^{-1} resolution with *b* polarization and $\mathbf{k}\|\mathbf{a}$.

the 44-cm^{-1} line. That line splits in a magnetic field as shown in Fig. 4 due to the splitting of the excited triplet state. It is also ten times stronger than the magnetic dipole transition at 15 cm^{-1}, and as our study has shown, is induced when $\mathbf{k}\|\mathbf{a}$ with *b* polarization only. If the Zn-induced features are electronic electric-dipole transitions, it is unclear which states could be involved. Since they are not split by a magnetic field, they are unlikely to involve transitions to or from triplet states. In-gap states, predicted by Martins *et al.*,[24] are also excluded because they would be absent above the SP transition temperature.

Local vibronic modes are another possibility. For a pure Zn translational mode for $x=0.003$ Zn we estimate a spectral weight of 530 cm^{-2} from the plasma frequency $\omega_p=(4\pi nZ^2e^2/M)^{1/2}=13$ cm^{-1} where *n* is the Zn concentration, *M* the mass of the Zn ion, and *Z* the effective charge that we take to be $+2$. This is over five times larger than the observed spectral weight. It is therefore likely that the mode also involves motion of other atoms.

The three-level system shown in Fig. 3 can be modeled with a square well with a central barrier. Appropriate choice of parameters gives levels at 10, 30, and 55 cm^{-1} above the ground state. Electric-dipole transitions between adjacent levels will give lines at 10, 20, and 25 cm^{-1}. The line at 25 cm^{-1} could very well be present in our spectra and account for the apparent broadening with temperature of the 20-cm^{-1} line. In general, the addition of the level at 55 cm^{-1} will improve the agreement between the calculated and observed temperature dependence of the line intensities shown in the lower panel of Fig. 3. The broadening of the 10- and 20-cm^{-1} lines with increased doping can be explained as being due to a long range of interaction between the defects.

The combination of a low intensity, a flat very anharmonic potential, and a polarization in the *ab* plane suggests that the lines at 10 and 20 cm^{-1} involve the Zn defect and the libration about the **c** axis of the surrounding four GeO_4 tetrahedra as shown in Fig. 1. In the undoped material the 48-cm^{-1} phonon is a similar mode that is optically active[6] and involves the motion of the Cu in the direction of the apical oxygens. With Cu replaced by Zn this mode would have a polarization with both **a** and **b** direction components and is consistent with the model of a potential well with a central barrier. Since Zn is known to favor a higher coordination number than Cu it will have a tendency to move off center towards one of the apical oxygens.

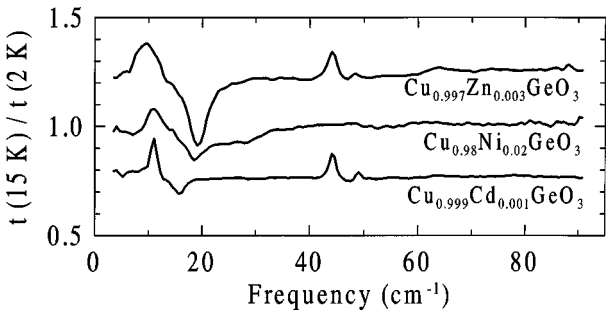

FIG. 5. Transmittance at 15 K divided by transmittance at 2 K of $x=0.003$ Zn-doped, 0.02 Ni-doped, and 0.001 Cd-doped $CuGeO_3$ with the Zn and Cd data offset for clarity. Lines similar to those at 10 and 20 cm^{-1} in the Zn-doped sample can also be seen in the Ni- and Cd-doped samples.

Libration of GeO_4 tetrahedra is also a component of the *static* SP distortion in the undoped material,[3,25] but it is not optically active since it involves odd combinations of the rotations of the GeO_4 tetrahedra and no displacement of the copper in the *ab* plane. In our picture the Zn doping has the effect of moving the mode at 48 cm^{-1} to 10 cm^{-1} by a dramatic reduction of the already weak restoring force for displacements of the planar oxygens in the direction of the apical oxygens around the Zn.

The identity of the ion that replaces the copper, however, does not appear to be critical since similar absorption lines are seen in Ni- and Cd-doped samples. Figure 5 shows transmittance at 15 K divided by transmittance at 2 K for samples with the three dopants. Where the Zn-doped sample has lines at 10 and 20 cm^{-1}, the Cd-doped sample has lines at 11 and 16 cm^{-1}, and the Ni-doped sample has lines at 11 and 18 cm^{-1}. These variations are surprisingly small considering the significantly larger size of the Cd^{2+} ion and the difference in the magnetic character of the Ni^{2+} ion that has spin $S=1$ instead of $S=0$. This insensitivity to the dopant ion suggests that the vibration is dominated by the relatively massive GeO_4 tetrahedra.

In contrast to the large changes in dynamics caused by dopants on the Cu sites, the replacement of Ge by Si will have the minor effect of reducing the size of one of the tetrahedra thereby affecting four Cu sites equally and, by symmetry, giving rise to a low-frequency optical mode polarized in the **b** direction. We observe no such mode in our Si-doped samples between 3 and 100 cm^{-1}.

One feature which remains to be explained is the 5–55-cm^{-1} band seen at higher doping levels. Its lower boundary is approximately defined by the 10-cm^{-1} line, and the upper boundary more or less coincides with the phonon at 48 cm^{-1}. The saturation of the absorption above a concentration of $x=0.02$ (inset to Fig. 2) is reminiscent of the phase diagram[8,11] in which T_N and T_{SP} stop changing at this same concentration. One explanation, suggested by the unusual flat shape of the band, is that it represents a disordered state of the local excitations as they begin to interact strongly at $x=0.02$ Zn and above. This state may also be relevant to the saturation of T_N and T_{SP} at the same doping level.

In summary, we have observed a low-lying lattice mode in Zn-, Cd-, and Ni-doped $CuGeO_3$ that we identify with the librational motion of GeO_4 tetrahedra combined with the displacement of the dopant ion in a very flat potential with a central barrier.

We acknowledge fruitful discussions with J. Barbier, D. B. Brown, B. Gaulin, and J. E. Greedan. The work at McMaster University and the University of Toronto was supported by NSERC of Canada and The Canadian Institute for Advanced Research. Work on correlated magnetic systems at Warwick is supported by a grant from the EPSRC of the U.K.

*Permanent address: National Institute of Chemical Physics and Biophysics, Akadeemia tee 23, Tallinn EE0026, Estonia.

[1] M. Hase, I. Terasaki, and K. Uchinokura, Phys. Rev. Lett. **70**, 3651 (1993).
[2] K. D. Hammonds, H. Deng, V. Heine, and M. T. Dove, Phys. Rev. Lett. **78**, 3701 (1997).
[3] K. Hirota, D. E. Cox, J. E. Lorenzo, G. Shirane, J. M. Tranquada, M. Haze, K. Uchinokura, H. Kojima, Y. Shibuya, and I. Tanaka, Phys. Rev. Lett. **73**, 736 (1994).
[4] P. H. M. van Loosdrecht, S. Huant, G. Martinez, G. Dhalenne, and A. Revcolevschi, Phys. Rev. B **54**, R3730 (1996).
[5] T. M. Brill, J. P. Boucher, J. Voiron, G. Dhalenne, A. Revcolevschi, and J. P. Renard, Phys. Rev. Lett. **73**, 1545 (1994).
[6] Z. V. Popović, S. D. Dević, V. N. Popov, G. Dhalenne, and A. Revcolevschi, Phys. Rev. B **52**, 4185 (1995).
[7] J.-G. Lussier, S. M. Coad, D. F. McMorrow, and D. McK. Paul, J. Phys.: Condens. Matter **7**, L325 (1995).
[8] Y. Sasago, N. Koide, K. Uchinokura, M. C. Martin, M. Hase, K. Hirota, and G. Shirane, Phys. Rev. B **54**, R6835 (1996).
[9] M. Hase, K. Uchinokura, R. J. Birgeneau, K. Hirota, and G. Shirane, J. Phys. Soc. Jpn. **65**, 1392 (1996).
[10] P. Fronzes, M. Poirier, A. Revcolevschi, and G. Dhalenne, Phys. Rev. B **55**, 8324 (1997).
[11] M. C. Martin, M. Hase, K. Hirota, G. Shirane, Y. Sasago, N. Koide, and K. Uchinokura, Phys. Rev. B **56**, 3173 (1997).
[12] J. P. Renard, K. Le Dang, P. Veillet, G. Dhalenne, A. Revcolevschi, and L.-P. Regnault, Europhys. Lett. **30**, 475 (1995).
[13] L. P. Regnault, J. P. Renard, G. Dhalenne, and A. Revcolevschi, Europhys. Lett. **32**, 579 (1995).
[14] M. Poirier, R. Beaudry, M. Castanguay, M. L. Plumer, G. Quirion, F. S. Razavi, A. Revcolevschi, and G. Dhalenne, Phys. Rev. B **52**, R6971 (1995).
[15] S. Coad, J.-G. Lussier, D. F. McMorrow, and D. McK. Paul, J. Phys.: Condens. Matter **8**, 6251 (1996).
[16] N. Koide, Y. Uchiyama, T. Hayashi, T. Masuda, Y. Sasago, K. Uchinokura, K. Manabe, and H. Ishimoto, cond-mat/9805095 (unpublished).
[17] A. Damascelli, D. van der Marel, F. Parmigiani, G. Dhalenne, and A. Revcolevshi, Phys. Rev. B **56**, R11 373 (1997).
[18] A. Damascelli, D. van der Marel, F. Parmigiani, G. Dhalenne, and A. Revcolevschi, Physica B **244**, 114 (1998).
[19] Design of the far-infrared spectrometer will be published later.
[20] H. Völlenkle, A. Wittmann, and H. Nowotny, Monatsch. Chem. **98**, 1352 (1967).
[21] We define spectral weight (in units of cm^{-2}) as $\int_0^\infty \alpha d\nu = (\pi^2/n)\omega_p^2$, where the absorption constant α, the frequency ν, and the plasma frequency ω_p are in units of cm^{-1} and n is the index of refraction.

[22] M. Hase, I. Terasaki, K. Uchinokura, M. Tokunaga, N. Miura, and H. Obara, Phys. Rev. B **48**, 9616 (1993).
[23] V. Kiryukhin, B. Keimer, J. P. Hill, S. M. Coad, and D. McK. Paul, Phys. Rev. B **54**, 7269 (1996).
[24] G. B. Martins, E. Dagotto, and J. A. Riera, Phys. Rev. B **54**, 16 032 (1996).
[25] M. Braden, G. Wilkendorf, J. Lorenzana, M. Aïn, G. J. McIntyre, M. Behruzi, G. Heger, G. Dhalenne, and A. Revcolevschi, Phys. Rev. B **54**, 1105 (1996).